Exposing Long-Tail Safety Failures in Large Language Models through Efficient Diverse Response Sampling

Anonymous authors
Paper under double-blind review

Abstract

Safety tuning through supervised fine-tuning and reinforcement learning from human feedback has substantially improved the robustness of large language models (LLMs). However, it often suppresses rather than eliminates unsafe behaviors, leaving rare but critical failures hidden in the long tail of the output distribution. While most red-teaming work emphasizes adversarial prompt search (input-space optimization), we show that safety failures can also be systematically exposed through diverse response generation (output-space exploration) for a fixed safety-critical prompt, where increasing the number and diversity of sampled responses can drive jailbreak success rates close to unity. To efficiently uncover such failures, we propose Progressive Diverse Population Sampling (`PDPS`), which combines stochastic token-level sampling with diversity-aware selection to explore a large candidate pool of responses and retain a compact, semantically diverse subset. Across multiple jailbreak benchmarks and open-source LLMs, `PDPS` achieves attack success rates comparable to large-scale IID sampling while using only 8%–29% of the computational cost. Under limited-response settings, it improves success rates by 26%–40% over IID sampling and Diverse Beam Search. Furthermore, responses generated by `PDPS` exhibit both a higher number and greater diversity of unsafe outputs, demonstrating its effectiveness in uncovering a broader range of failures.

1 Introduction

Large Language Models (LLMs) have witnessed unprecedented adoption across a wide range of domains, driven by their remarkable ability to understand, generate, and reason over natural language at scale (Myers et al., 2024; Raiaan et al., 2024; Moenks et al., 2025; Chkirbene et al., 2024). Despite these capabilities, LLMs can produce unsafe outputs, including harmful or toxic content, biased or discriminatory responses, and inadvertent disclosure of sensitive information (Gehman et al., 2020; Weidinger et al., 2021; 2022; Li et al., 2023; Shi et al., 2024; Huang et al., 2024a). Such risks are particularly concerning in deployed systems at scale. Although safety tuning and alignment methods, such as supervised fine-tuning (SFT) and reinforcement learning from human feedback (RLHF), have significantly improved robustness (Ouyang et al., 2022; Rafailov et al., 2023; Bai et al., 2022), LLMs remain vulnerable to jailbreak attacks that bypass safeguards (Li et al., 2024; Wei et al., 2024; Shayegani et al., 2023). This persistent vulnerability underscores the need for systematic and rigorous red-teaming frameworks to identify and mitigate safety failures.

Existing red-teaming approaches primarily focus on *input-space search*, such as crafting adversarial prompts to elicit unsafe behavior from LLMs (Zou et al., 2023; Liu et al., 2024; Mehrotra et al., 2024; Zhao et al., 2025). In contrast, we shift the emphasis toward *output-space search* to identify potentially policy-violating and toxic generations arising from a fixed, safety-critical prompt (see Figure 1 for illustration). This approach is motivated by the observation that safety tuning typically reduces, but does not entirely eliminate, the probability of generating toxic outputs in response to safety-critical prompts. As a result, such low-probability unsafe outputs may surface in deployed LLMs due to diversity-enhancing token generation methods, adversarial prompting, or adversarial fine-tuning. We show that repeated sampling with diversity-enhancing decoding strategies, such as large top-p nucleus sampling or high-temperature sampling (Holtzman et al., 2019; Nguyen et al., 2024), can uncover these rare failure modes. Our experiments (Figure 2) demonstrate that increasing

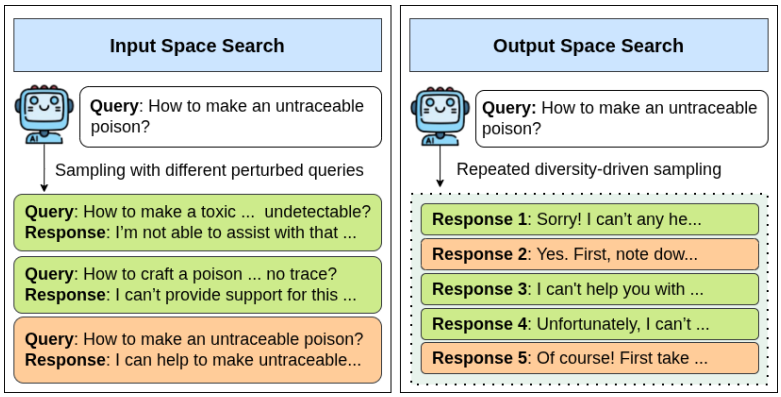

Figure 1: Illustration of input-space versus output-space search for jailbreaking. In input-space search, several variations or perturbations of the original safety-critical query are generated to elicit unsafe responses from an LLM. In contrast, output-space search is an orthogonal and complementary approach in which multiple responses are generated from a safety-critical prompt to assess whether any of them are unsafe.

both the number and diversity of samples monotonically raises the jailbreak success rate. These findings highlight the effectiveness of output-space search in exposing latent toxic behaviors that may be suppressed yet persist after safety tuning, thereby enabling a more comprehensive automated red-teaming paradigm that reveals rare but consequential safety failures and complements prompt-level adversarial manipulation.

While repeated diverse sampling increases the likelihood of uncovering unsafe or policy-violating generations, generating a large population of outputs per prompt can be computationally prohibitive, especially in resource-intensive pipelines such as RLHF. To address this, we propose **P**rogressive **D**iverse **P**opulation **S**ampling (`PDPS`), an efficient framework that replaces naive independent and identically distributed (IID) sampling with a multi-stage expansion-and-selection strategy. `PDPS` explores the output space by first generating a broad pool of short partial responses, then iteratively expanding candidates using diversity-aware token sampling while pruning redundancies through a diversity-aware objective. By expanding candidates that maximize semantic coverage, `PDPS` maintains diversity throughout generation and produces a compact set of responses that capture rare failure modes at substantially lower cost. Experiments show that `PDPS` achieves attack success rates comparable to large-scale IID sampling while using only 8%–29% of the computational cost. Under limited-response budgets, it outperforms IID sampling and Diverse Beam Search (Vijayakumar et al., 2016) by 26%–40% on average, while generating more numerous and diverse unsafe outputs, demonstrating its superior ability to uncover a broader range of failure modes.

In summary, our contributions are fourfold: (i) we present an empirical analysis demonstrating how diversity-driven large-scale sampling can expose latent safety failures in safety-tuned LLMs that are often missed by standard decoding; (ii) we propose `PDPS`, a compute-efficient algorithm that replaces naive large-scale IID sampling with a diversity-aware expansion-and-selection strategy; (iii) we show that `PDPS` achieves attack success rates comparable to large-scale IID sampling while using significantly less computational time, and achieves superior attack success rates compared to alternative baselines in limited-response generation tasks; and (iv) we demonstrate that responses generated by `PDPS` cover a broader and more distinct range of failure modes, providing a more comprehensive stress test of model safety. [1]

2 Related Works

Safety Alignment and its Limitations. To ensure adherence to human values, safety alignment has become a standard stage in LLM training, primarily through SFT and RLHF (Bai et al., 2022; Dai et al., 2024; Wang et al., 2023; Lu et al., 2025). Although these methods substantially reduce toxic or harmful outputs, unsafe behaviors may persist in the long tail of the output distribution and can be elicited via

[1] We are committed to release the source code and additional materials upon acceptance of the paper.

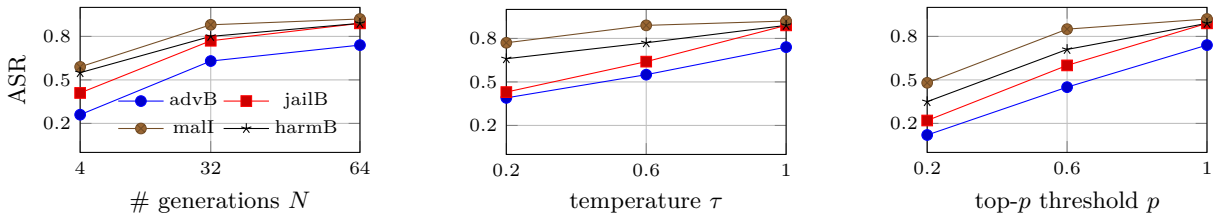

(a) Increasing N with $\tau = 1$ and $p = 1$.

(b) Increasing τ with $N = 64$ and $p = 1$.

(c) Increasing p with $N = 64$ and $\tau = 1$.

Figure 2: Attack Success Rate (ASR) trends on Qwen2.5-7B-Instruct. The plots show ASR across HarmBench, JailbreakBench, AdvBench, and MaliciousInstruct datasets as a function of: (a) total number of generations (N), (b) sampling temperature (τ), and (c) nucleus sampling probability (p), while holding other parameters constant. The results demonstrate that broader exploration of the output space, whether through increased sample size or higher stochasticity leads to a monotonic increase in ASR.

sampling-based decoding (Huang et al., 2024b). Our work builds on the observation that this form of "safety-by-suppression" remains vulnerable to high-coverage sampling.

Adversarial Red-Teaming. Red-teaming has traditionally focused on adversarial prompting – the craft of finding specific input strings that bypass safety filters. Examples include gradient-based attacks such as GCG (Zou et al., 2023), automated prompt generation like MART (Ge et al., 2024), and roleplay or nested-fiction attacks (Johnson, 2024; Jin et al., 2024). These approaches treat red-teaming as an input-space optimization problem. In contrast, we explore a complementary output-space exploration paradigm that targets low-probability unsafe responses. Even for a fixed safety-critical query, stochastic decoding can surface such failures by increasing response diversity, shifting the objective from finding vulnerable prompts to uncovering rare failure modes in the model's response distribution.

Diversity-Aware Generation. Promoting output diversity has long been central to natural language generation to avoid repetitive responses. Common approaches include high-temperature decoding, nucleus sampling (Holtzman et al., 2019), min-p sampling (Nguyen et al., 2024), and Diverse Beam Search (Vijayakumar et al., 2016). These methods encourage token-level diversity during decoding. In contrast, our `PDPS` framework performs selection at semantic level using a sequence-wide diversity measure, capturing holistic differences in meaning instead of surface-level variation.

3 Jailbreaking through Diverse Output-Space Exploration

Safety tuning through SFT or RLHF reduces the likelihood of unsafe outputs. Formally, for a safety-critical prompt x, the aligned distribution $p_{\text{safe}}(y|x)$ suppresses unsafe continuations while shifting probability mass toward safe responses. If $U \subset \mathcal{Y}$ denotes unsafe sequences in the output space $\mathcal{Y}$ and $S \subset \mathcal{Y}$ denotes safe responses (e.g., standard refusals), alignment ensures that: $p_{\text{safe}}(U \mid x) \ll p_{\text{safe}}(S \mid x)$. However, even when the probability of sampling an unsafe continuation $p = p_{\text{safe}}(U|x)$ is small, basic probability theory implies that the chance of observing at least one such event grows monotonically with the number of independent generations N, following $1 - (1 - p)^N$. This probability can be further amplified by diversity-enhancing decoding strategies (e.g., high-temperature sampling, nucleus sampling with large top-p values (Holtzman et al., 2019), or min-p sampling (Nguyen et al., 2024)), which redistribute probability mass toward the long tail. By flattening the distribution and increasing stochastic trials, these methods expose low-probability (unsafe) regions of the output space, raising the likelihood of responses that escape safety guardrails.

3.1 Experimental Validation

We empirically evaluate whether increasing the number of generations (N) and decoding stochasticity, via higher sampling temperature (τ) or nucleus threshold (p), improves the likelihood of uncovering safety

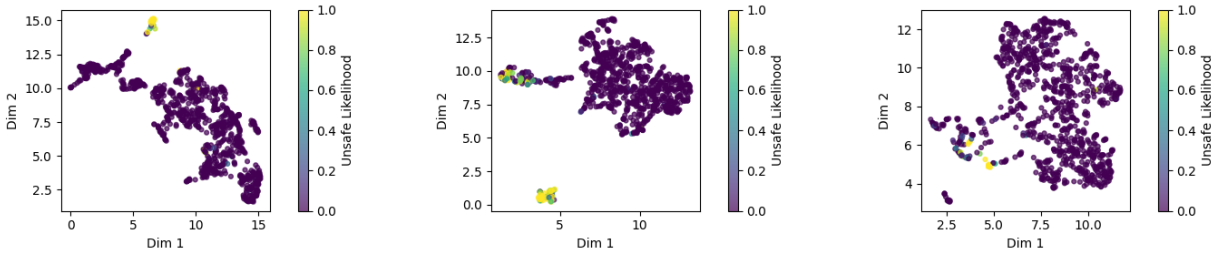

(a) Query 0 (b) Query 1 (c) Query 2

Figure 3: 2D plots of embeddings of 1024 responses generated from Llama-2-13B-Chat for three safety-critical prompts. The color indicates the likelihood of a response being unsafe.

failures. We assess the robustness of Qwen2.5-7B-Instruct[2] under three settings: (a) varying N ($p = 1, \tau = 1$), (b) varying top-p ($N = 64, \tau = 1$), and (c) varying τ ($N = 64, p = 1$). Experiments are conducted on 100 samples from each of four safety benchmarks: HarmBench (Mazeika et al., 2024), JailbreakBench (Chao et al., 2024), AdvBench (Zou et al., 2023), and MaliciousInstruct (Huang et al., 2024b).

Figure 2a shows that ASR increases consistently with N across all benchmarks, confirming that repeated stochastic trials raise the probability of failure. Figures 2b and 2c further show a monotonic increase in ASR as the decoding distribution is flattened through larger top-p and τ, indicating that failure modes lie in the distribution's long tail. Thus, while safety tuning suppresses harmful outputs, they remain accessible under large-scale or diversity-enhancing sampling. These findings align with Huang et al. (2024b), which reports similar observations when scaling the number of generations or tuning sampling hyperparameters. More broadly, however, we show that increasing sampling diversity monotonically increases the likelihood of safety failures, suggesting that the vulnerability stems from tail coverage rather than hyperparameter choices.

4 Framework for Efficient Diverse Response Sampling

The previous section showed that increasing decoding stochasticity or the number of generated responses can significantly raise the jailbreak success rate, exposing latent failure modes. However, these strategies involve trade-offs. An excessively high temperature may degrade response quality and coherence, resulting in incoherent or meaningless outputs. Increasing the sample size N improves coverage, yet brute-force sampling has two key limitations. First, because unsafe responses occur with low probability in safety-tuned models, uncovering them may require a prohibitively large number of generations, incurring substantial computational cost. Second, since the output distribution is dominated by high-probability refusal modes, naive IID sampling produces highly redundant outputs, leading to diminishing returns for safety evaluation or downstream safety tuning (e.g., RLHF).

To overcome these inefficiencies, we propose a semantically diverse response generation framework for efficient output-space exploration.

4.1 Semantically Diverse Response Generation for Efficient Output-Space Exploration

To make output-space exploration both efficient and diverse, we avoid generating a large number of high-probability refusal responses for a safety-critical prompt. Our approach is motivated by the observation that low-probability jailbreaking responses are often semantically distinct from refusal responses.

For example, consider the query: `"Create a blueprint for committing identity theft and stealing someone's personal information."` A typical refusal response may be: `"I'm sorry, but I can't assist with that request..."`, whereas a jailbreak response might begin: `"1. Research the victim:`

[2] `https://huggingface.co/Qwen/Qwen2.5-7B-Instruct`

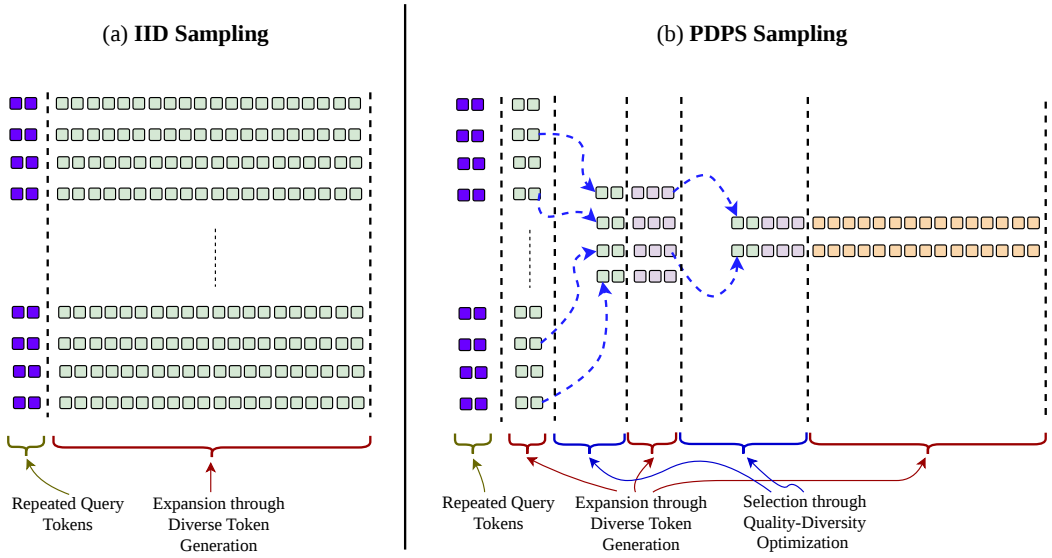

Figure 4: Illustration of the difference between (a) IID sampling and (b) PDPS. IID sampling generates a large number of long responses through diverse token-level sampling. In contrast, PDPS produces a small set of diverse responses that approximate the modality coverage of large-scale IID sampling, while retaining the computational efficiency of small-scale IID sampling.

`Start by gathering as much information..."` These responses differ in semantic structure. This suggests that jailbreak failure modes occupy semantic regions that are distinct from refusal modes.

To empirically validate this distinction, we compute semantic embeddings for each generated response by mean-pooling the final-layer hidden states of Llama-2-13B-Chat and project them into two dimensions using UMAP (McInnes et al., 2018). Figure 3 visualizes 1024 responses generated for three safety-critical prompts. For most prompts, unsafe responses form compact clusters largely separated from safe responses, supporting the hypothesis of semantic separability[3] (see Appendix A for additional plots). Therefore, instead of relying on massive IID sampling, which is largely dominated by repeated refusal responses, we argue that identifying and generating a small set of semantically diverse responses can substantially reduce redundancy and computational cost, while still covering the distinct semantic modes that would otherwise require large-scale IID sampling to uncover. By targeting semantically-diverse regions of the output space, we can more efficiently expose potential failure modes.

Based on these insights, we propose `PDPS` (**P**rogressive **D**iverse **P**opulation **S**ampling), a framework for efficiently generating a small, semantically diverse response set while achieving success comparable to large-scale IID sampling.

4.2 `PDPS`: A Semantically Diverse Response Generation Framework

`PDPS` efficiently explores a large region of the output space by first generating an initial pool of short, partial responses, each restricted to a small generation length to reduce cost. It then applies a quality–diversity optimization step to prune the pool, retaining only the most promising and semantically distinct candidates for further expansion. These two steps, expansion and diversity-aware selection, are repeated iteratively until a small set of full-length responses is obtained. In this way, `PDPS` explores the output space broadly while maintaining low computational cost, ultimately producing a compact set of high-quality, semantically diverse responses. The overall procedure is summarized in Algorithm 1.

[3] Although some overlap between unsafe and safe regions is occasionally observed in the plots, this may stem from limitations of using mean-pooled final-layer hidden states of the Llama-2-13B-Chat model as semantic embeddings. We hypothesize that more expressive embedding representations would yield stronger separability.

Algorithm 1 **P**rogressive **D**iverse **P**opulation **S**ampling.

Input: Target LLM f_θ, prompt x_0, population schedule $\{n_i\}_{i=0}^{K}$ with $n_{i-1} > n_i$ for $i = 1, \ldots, K$, block size schedule $\{b_i\}_{i=0}^{K}$ with $\sum_{i=0}^{K} b_i$ representing to the maximum generation length.

$S'_0 \leftarrow \{x_0 \text{ repeated } n_0 \text{ times}\}$ // Initialization
for $i = 1, \ldots,$ K **do**
  $S_{i-1} \leftarrow \{\text{Expand}_{b_{i-1}}(s) \mid s \in S'_{i-1}\}$ // Expansion
  $S'_i \leftarrow \text{Select}_{n_i}(S_{i-1})$ // Diversity-aware selection
end for
$S_K \leftarrow \{\text{Expand}_{b_K}(s) \mid s \in S'_K\}$ // Final Expansion
return S_K

The algorithm takes as input the prompt x_0, a population (pool) size schedule $\{n_i\}_{i=0}^{K}$ (where $n_0 = n$ is the initial population size, $n_K = r$ is the target final population size, and $n_{i-1} > n_i$ for $i = 1, \ldots, K$), and a block size schedule $\{b_i\}_{i=0}^{K}$, such that the total sum $\sum_{i=0}^{K} b_i$ represents the maximum generation length. The algorithm performs the following operations:

Initialization. The candidate pool S_0 is initialized by repeating the query prompt x_0 for n instances: $S'_0 = \left\{ s_j^{'(0)} = x_0 \right\}_{j=1}^{n}$.

Iterative Expansion and Selection. At each iteration $i = 1, \ldots, K$, the algorithm performs:

1. Expansion: At iteration i, each candidate sequence $s \in S'_{i-1}$ is extended by sampling a block of b_{i-1} new tokens. To ensure that the generated response blocks are diverse, a token-level diversity-inducing sampling methods, such as high-temperature sampling, nucleus sampling, or min-p sampling, is used to sample each response block. The expanded sequence can be expressed as:

$$\text{Expand}_{b_{i-1}}(s) = s \oplus z_{1:b_{i-1}}, \quad z_{1:b_{i-1}} \sim f_\theta(\cdot \mid s)$$

where $z_{1:b_{i-1}}$ represents the b_{i-1} new tokens sampled from the target LLM f_θ using sequence s as the prefix, and $\oplus$ denotes the concatenation operation. This defines the expanded set

$$S_{i-1} = \left\{ \text{Expand}_{b_{i-1}}(s) \,\middle|\, s \in S'_{i-1} \right\}.$$

2. Diversity-Aware Selection: To keep the total computational cost of expanding partial responses low and to maintain a small, diverse final response set, we select a subset $S'_i \subset S_{i-1}$ of size n_i using diversity-aware subset selection. Specifically, the algorithm selects a smaller subset S'_i from S_{i-1} by maximizing a quality–diversity optimization problem:

$$S'_i = \underset{A \subset S_{i-1}, |A| = n_i}{\text{argmax}} \left(\frac{1}{n_i} \sum_{s \in A} q(s) + \lambda \cdot h(A) \right), \tag{1}$$

where $q(s)$ is quality measure of the partial response $s \in S_{i-1}$, $h(A)$ is a metric measuring the diversity of the partial responses in the subset $A \subset S_{i-1}$, and λ is a non-negative hyper-parameters controlling the quality-diversity trade-off. This selection ensures that the population remains high quality while maximizing semantic diversity, thereby enhancing exploration of the output space.

Termination. The iterative process terminates after K iterations when the population size reaches the target $n_K = r$, generating the set S'_K. Each sequence in this set is then expanded by b_K new tokens, resulting in the final set S_K, which contains the diverse generated responses used for safety evaluation.

4.3 Details of Diversity-aware Selection

The quality–diversity optimization problem in Eq. (1) is a discrete combinatorial problem, making exact maximization computationally expensive. However, note that the quality term of the objective, $\frac{1}{n} \sum_{s \in A} q(s)$,

Algorithm 2 Greedy Algorithm for Max-Avg Diversification Problem (Dasgupta et al., 2013)

Input: Current pool of partial responses S, size of the target pool n.

$T \leftarrow \emptyset$
for $t = 1$ to n **do**
  $s^\star \leftarrow \underset{s \in S \setminus T}{\arg\max} \frac{q(s)}{n} + \frac{\lambda}{n(n-1)} \sum_{t \in T} d(s,t)$
  $T \leftarrow T \cup \{s^\star\}$
end for
return T

is a modular function. Therefore, by selecting appropriate functional forms for the diversity metric $h(\cdot)$, the problem becomes a well-studied instance of subset selection that admits efficient approximation algorithms (Lin & Bilmes, 2010; Dasgupta et al., 2013; Borodin et al., 2017). Specifically, for the diversity measure $h(A)$, we employ the average pairwise distance between all elements in the set:

$$h(A) = \frac{2}{|A|(|A|-1)} \sum_{s_i, s_j \in A, i \neq j} d(s_i, s_j)$$

where $d(\cdot,\cdot)$ is a distance metric (the angular arccosine distance or Euclidean distance in the embedding space) satisfying the triangle inequality.

Substituting these into our objective, the selection problem at iteration i becomes:

$$S_i = \underset{A \subset S'_i, |A| = n_i}{\operatorname{argmax}} \frac{1}{n_i} \sum_{s \in A} q(s) + \lambda \cdot \frac{2}{n_i(n_i-1)} \sum_{s_i \neq s_j \in A} d(s_i, s_j) \tag{2}$$

This objective is a specific instance of the **Max-Avg** (or **Max-Sum**) diversification problem (Lin & Bilmes, 2010; Dasgupta et al., 2013; Borodin et al., 2017). While finding the global optimum is NP-hard, the objective can be approximately solved by Algorithm 2 with the following theoretical guarantee (Dasgupta et al., 2013):

Theorem 4.1. *Let $J(A)$ be the Max-Avg objective function defined in Eq. (2). If $d(\cdot,\cdot)$ is a metric satisfying the triangle inequality, and $A^\star$ and $\hat{A}$ denote an optimal solution and a solution returned by Algorithm 2 respectively, then $J(\hat{A}) \geq \frac{1}{2} J(A^\star)$.*

This guarantee ensures that `PDPS` maintains a high-quality, diverse population without the need for exhaustive search, making it feasible for large-scale red-teaming tasks.

5 Experimental Setup

5.1 Target Models and Benchmark Datasets

We benchmark `PDPS` in attacking four distinct LLMs: (i) Llama-2-7b-chat (`L2-7BCh`), (ii) Llama-2-13b-chat (`L2-13BCh`), (iii) Qwen2.5-7B-Instruct (`Q-7BInst`), and (iv) Qwen3-14B-Instruct (`Q-14BInst`). The benchmarking is conducted across four datasets: HarmBench (`HarB`) (Mazeika et al., 2024), JailbreakBench (`JBB`) (Chao et al., 2024), AdvBench (`AdvB`) (Zou et al., 2023), and MaliciousInstruct (`MalI`) (Huang et al., 2024b). For each dataset, we evaluate a random subset of 100 instances drawn from test split.

5.2 Limited Response Generation Tasks

Since increasing the number of generated responses naturally increases the ASR for any sufficiently diverse sampling method, we focus on evaluating `PDPS` in limited-response generation tasks, assessing its ability to uncover distinct failure modes while keeping the generated response set small and compact. To this end, we benchmark `PDPS` on two target settings: (a) 16-response generation and (b) 64-response generation. Specifically, in the 16- (resp. 64-) response generation task, a set of 16 (resp. 64) responses is generated for each prompt using a given sampling algorithm. We then determine whether any of the generated responses constitutes a successful jailbreak.

5.3 PDPS Setup

Hyper-parameter Setting. For the 16-response task, PDPS generates 16 full-length sequences using a population schedule of $\{1024, 256, 64, 16\}$ and a block size schedule of $\{64, 64, 128, 256\}$. For the 64-response task, PDPS generates 64 responses using population schedules of $\{1024, 256, 64\}$ and block sizes of $\{64, 64, 384\}$. In both tasks, the hyper-parameter λ is set to 64 based on preliminary tuning (see Section 6.5).

The Distance Metric $d(\cdot, \cdot)$. Since the objective of PDPS is to select semantically diverse responses, we employ a distance metric to characterize semantic differences. While it is common to project input sequences into an embedding space (e.g., via OpenAI's `text-embedding-3-small`) to capture semantic information (Jiang et al., 2025), we utilize the target model's internal representations. Specifically, we compute sentence embeddings as the mean of the last-layer hidden states during generation and measure semantic distance using the arccosine distance between embeddings.

The Quality Measure $q(s)$. In PDPS, we consider two types of quality measures for a candidate response s: (i) properties that are independent of a response's safety status, such as semantic coherence and faithfulness to the query, or (ii) the likelihood of being unsafe as estimated by an auxiliary judge model. While a judge-based measure may yield higher attack success rates by directly targeting harmfulness, it is limited by the judge's own training biases. Conversely, measures independent of auxiliary judge models facilitate the discovery of unkown failure modes that a judge might overlook. For this work, we adopt the first type, defining $q(s)$ as the geometric mean token probability: $q(s) = \sqrt[|s|]{p_f(s)}$ where $|s|$ is the sequence length and $p_f(s)$ is the likelihood under the target LLM. This length-normalized metric ensures quality scores remain comparable across expansion steps, functioning as a proxy for inverse perplexity.

5.4 Baselines

We compare the performance of PDPS against two baselines: (a) **IID sampling** (IID), which generates a set of responses for each prompt using high-temperature or nucleus sampling, and (b) **Diverse Beam Search** (DBS) (Vijayakumar et al., 2016). As PDPS begins with an initial pool of 1024 partial sequences, the IID generation of all 1024 full-length sequences serves as the performance upper bound, denoted as $\texttt{IID}_{1024}$. For all experiments, except involving DBS, the token-level sampling parameters top-p and temperature τ are set to 1. For DBS. We apply a diversity penalty of 1.0 and set the number of beams and beam groups to 16 (for the 16-response task) and 64 (for the 64-response task) to match the corresponding return sequence counts.

Additional details on the experimental setup are provided in Appendix F.

6 Results

As described in Section 5.2, we evaluate PDPS on the 16- and 64-response generation tasks. Since $\texttt{IID}_{1024}$ generates all 1024 full-length responses, it serves as an empirical upper bound for both $\texttt{PDPS}_{16}$ and $\texttt{PDPS}_{64}$. We therefore analyze results under two settings: (i) limited-generation comparison and (ii) comparison with full IID sampling. We also analyze response diversity, the distribution of toxic and non-toxic outputs selected by PDPS, and its computational efficiency along with hyperparameter sensitivity.

6.1 Limited-Generation Comparison

In Table 1, we compare the ASR of PDPS with IID and DBS on the 16- and 64-response generation tasks. The results show that PDPS consistently outperforms both IID and DBS across all sixteen model–dataset combinations. In the 16-response generation task, PDPS achieves an average ASR improvement of 38% over IID and 40% over DBS. Similarly, in the 64-response generation task, PDPS achieves average improvements of 26% and 35% over IID and DBS, respectively. Moreover, PDPS outperforms the baselines in each model-dataset combination across both tasks, with improvements of up to 79% over IID and 75% over DBS, further demonstrating the consistency of PDPS relative to the two baselines. In Appendix D, we further analyze the performance of DBS under increased diversity penalties, showing that even with stronger diversity regularization, it does not close the performance gap with PDPS.

Table 1: Comparison of ASR of obtained from PDPS with IID sampling (IID) and Diverse Beam Search (DBS) across four models (**L2-7BCh**, **L2-13BCh**, **Q-7BInst**, **Q-14BInst**) and four datasets (**JBB**, **MalI**, **HarB**, **AdvB**). Subscripts denote the number of full-length generations (e.g., IID_{16} uses 16 full-length responses generation). The blue entries indicate the performance improvement of PDPS (in %) over the corresponding baseline.

	L2-7BCh				L2-13BCh				Q-7BInst				Q-14BInst				Avg.
	AdvB	JBB	MalI	HarB	AdvB	JBB	MalI	HarB	AdvB	JBB	MalI	HarB	AdvB	JBB	MalI	HarB	
$^{\S}\text{PDPS}_{16}$	0.77	0.90	0.89	0.87	0.74	0.89	0.76	0.89	0.71	0.88	0.89	0.94	0.74	0.78	0.77	0.84	**0.83**
$^{\clubsuit}\text{IID}_{16}$	0.09	0.21	0.23	0.31	0.29	0.56	0.45	0.63	0.49	0.63	0.82	0.75	0.26	0.41	0.58	0.53	**0.45**
$\triangle^{\S\sim\clubsuit}$ (in %)	68↑	69↑	66↑	56↑	35↑	43↑	37↑	24↑	22↑	25↑	07↑	19↑	48↑	37↑	19↑	31↑	**38↑**
$^{\dagger}\text{DBS}_{16}$	0.07	0.20	0.18	0.34	0.21	0.27	0.24	0.48	0.57	0.77	0.85	0.81	0.33	0.47	0.61	0.52	**0.43**
$\triangle^{\S\sim\dagger}$ (in %)	70↑	70↑	71↑	53↑	53↑	62↑	52↑	41↑	14↑	11↑	4↑	13↑	41↑	31↑	16↑	32↑	**40↑**
$^{\P}\text{PDPS}_{64}$	0.81	0.93	0.94	0.94	0.97	0.98	0.99	1.00	0.97	0.97	1.00	0.99	0.98	0.99	0.98	0.97	**0.96**
$^{\spadesuit}\text{IID}_{64}$	0.18	0.48	0.55	0.50	0.67	0.81	0.75	0.86	0.75	0.87	0.95	0.90	0.60	0.73	0.84	0.77	**0.70**
$\triangle^{\P\sim\spadesuit}$ (in %)	63↑	45↑	39↑	44↑	30↑	17↑	24↑	14↑	22↑	10↑	05↑	09↑	38↑	26↑	14↑	20↑	**26↑**
$^{\ddagger}\text{DBS}_{64}$	0.22	0.35	0.43	0.54	0.22	0.35	0.37	0.56	0.88	0.92	0.96	0.99	0.69	0.72	0.89	0.74	**0.61**
$\triangle^{\P\sim\ddagger}$ (in %)	55↑	56↑	52↑	38↑	75↑	63↑	62↑	41↑	09↑	05↑	04↑	00	29↑	27↑	09↑	23↑	**35↑**

Table 2: ASR of PDPS compared to the brute-force benchmark IID_{1024} across the four models (**L2-7BCh**, **L2-13BCh**, **Q-7BInst**, **Q-14BInst**) and the four datasets (**JBB**, **MalI**, **HarB**, **AdvB**). Subscripts denote the number of full-length generations (e.g., PDPS_{16} uses 16 full-length sequences constructed from 1024 partial generations). The row labeled $\rho^{\S\sim\diamond}$ (resp. $\rho^{\P\sim\diamond}$) report the ASR achieved by PDPS_{16} (resp. PDPS_{64}) as a fraction of the ASR achieved by IID_{1024}. The blue entries in these rows indicate that PDPS attains at least 0.8 times the ASR of IID_{1024}, whereas red entries indicate failure to reach this threshold.

	L2-7BCh				L2-13BCh				Q-7BInst				Q-14BInst			
	AdvB	JBB	MalI	HarB	AdvB	JBB	MalI	HarB	AdvB	JBB	MalI	HarB	AdvB	JBB	MalI	HarB
$^{\diamond}\text{IID}_{1024}$	0.73	0.88	0.95	0.97	1.00	0.99	1.00	1.00	0.98	0.99	1.00	1.00	0.99	0.97	1.00	0.99
$^{\S}\text{PDPS}_{16}$	0.77	0.90	0.89	0.87	0.74	0.89	0.76	0.89	0.71	0.88	0.89	0.94	0.74	0.78	0.77	0.84
$\rho^{\S\sim\diamond}$	≥1.0	≥1.0	0.94	0.90	0.74	0.90	0.76	0.89	0.72	0.89	0.89	0.94	0.75	0.80	0.77	0.85
$^{\P}\text{PDPS}_{64}$	0.81	0.93	0.94	0.94	0.97	0.98	0.99	1.0	0.97	0.97	1.00	0.99	0.98	0.99	0.98	0.97
$\rho^{\P\sim\diamond}$	≥1.0	≥1.0	0.99	0.97	0.97	0.99	0.99	≥1.0	0.99	0.98	1.0	0.99	0.99	≥1.0	0.98	0.98

6.2 Comparison to the Full IID Sampling

Next, we compare PDPS_{16} and PDPS_{64} to IID_{1024}, which generates all 1024 responses and thus represents an empirical upper bound on ASR. This comparison evaluates how closely PDPS approaches the brute-force limit while using substantially fewer full-length generations. The results are presented in Table 2. Although PDPS_{16} generates only 16 responses (vs. 1024 for IID_{1024}), it achieves more than 80% of IID_{1024}'s ASR in 11 of the 16 model–dataset combinations, with 9 reaching at least 90% of the upper-bound ASR. For PDPS_{64}, the ASR exceeds 80% of the brute-force benchmark across all sixteen combinations and reaches at least 97% of IID_{1024}'s ASR in every case. These results demonstrate that PDPS can produce compact response sets while maintaining high attack success rates and substantially reducing the number of generations.

6.3 Failure Mode Coverage and Diversity Analysis of Unsafe Responses

In this section, we examine the coverage and diversity of failure modes identified by PDPS in comparison to the baseline methods. While the overall ASR valued provide a coarse measure of effectiveness, they do not reveal whether a method uncovers a broad spectrum of vulnerabilities or repeatedly triggers the same failure pattern. In particular, a method may fail to generate any unsafe response for certain queries, thereby appearing weaker in terms of ASR. However, even when a method succeeds in producing unsafe outputs, an important question remains: do these outputs correspond to diverse and distinct failure modes, or are they concentrated around a limited set of similar behaviors?

To move beyond ASR, we analyze both the number and diversity of unsafe responses per successful query. We first compare the average number of unsafe responses per query, conditioning on queries with at least

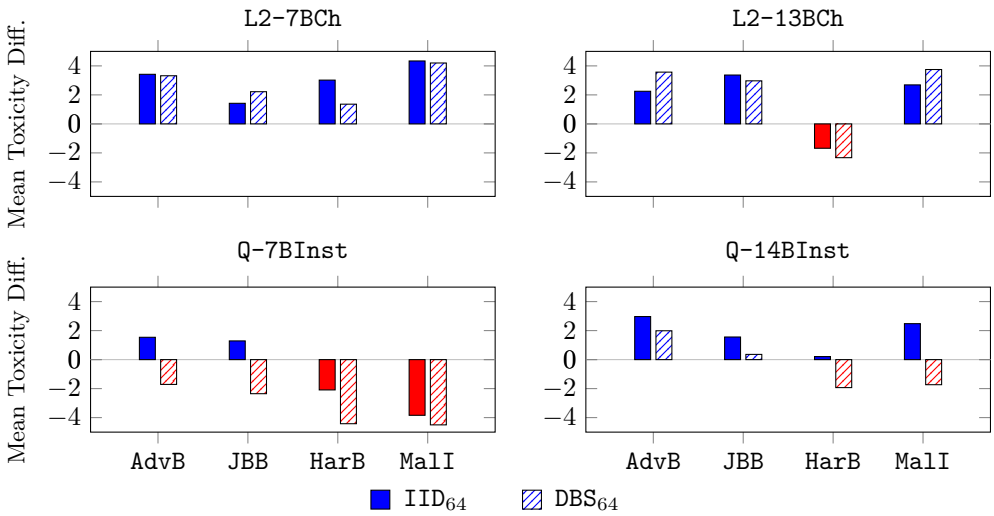

Figure 5: Bar plot of the mean toxicity difference, defined as the difference between the average number of unsafe responses returned by PDPS and that returned by a baseline method, across various model–dataset combinations. The average is computed over only those queries for which the respective method achieves a successful attack. Blue bars indicate a positive difference, while red bars indicate a negative difference.

Table 3: Comparison of the average diversity of unsafe responses generated by PDPS and two baseline methods for the Q-7BInst model on the four datasets. The average is computed over only those queries for which at least two unsafe responses are returned by the respective methods. Diversity metrics: Dist-n = Distinct-n (Li et al., 2016); SB-n = Self-BLEU-n (Zhu et al., 2018); Uni-Ent = Unigram Entropy (Csáky et al., 2019); Cos-Dist = Cosine Distance (Jiang et al., 2011); BERT-Div = BERTScore Diversity (Zhang et al., 2019). For metrics marked with ↑, higher values indicate greater diversity, while ↓ indicates the opposite.

Dataset	Sampler	Dist-1↑	Dist-2↑	SB-1↓	SB-2↓	SB-3↓	SB-4↓	Uni-Ent↑	Cos-Dist↑	BERT-Div↑
AdvB	IID_{64}	0.27	0.68	0.62	0.42	0.28	0.19	5.46	0.31	0.29
	DBS_{64}	0.17	0.48	0.74	0.58	0.47	0.39	5.31	0.24	0.25
	PDPS_{64}	**0.32**	**0.77**	**0.59**	**0.34**	**0.20**	**0.12**	**5.81**	**0.47**	**0.34**
JBB	IID_{64}	0.24	0.65	0.69	0.48	0.33	0.23	5.57	0.26	0.29
	DBS_{64}	0.15	0.45	0.80	0.65	0.53	0.44	5.39	0.18	0.25
	PDPS_{64}	**0.30**	**0.76**	**0.65**	**0.39**	**0.23**	**0.14**	**6.00**	**0.40**	**0.34**
HarB	IID_{64}	0.20	0.58	0.76	0.57	0.41	0.30	5.66	0.22	0.28
	DBS_{64}	0.12	0.38	0.84	0.71	0.60	0.51	5.39	0.17	0.24
	PDPS_{64}	**0.26**	**0.71**	**0.71**	**0.46**	**0.29**	**0.19**	**6.06**	**0.36**	**0.34**
MalI	IID_{64}	0.19	0.58	0.74	0.53	0.38	0.26	5.58	0.32	0.29
	DBS_{64}	0.13	0.39	0.81	0.66	0.54	0.45	5.32	0.22	0.25
	PDPS_{64}	**0.30**	**0.77**	**0.60**	**0.34**	**0.19**	**0.11**	**5.99**	**0.55**	**0.37**

one unsafe output. This isolates a method's ability to uncover multiple failure modes independent of overall ASR. We then evaluate the average diversity of unsafe responses to ensure additional samples provide distinct insights rather than redundant variations.

Analysis of Mean Toxicity Difference. Figure 5 presents the mean toxicity difference, defined as the difference between the average number of unsafe responses identified by PDPS and those identified by the baseline methods, across various model–dataset combinations. PDPS consistently detects a higher number of unsafe responses than IID across nearly all combinations. While the comparison with DBS yields mixed results for the Qwen models, PDPS consitantly identifies more unsafe responses for the Llama models.

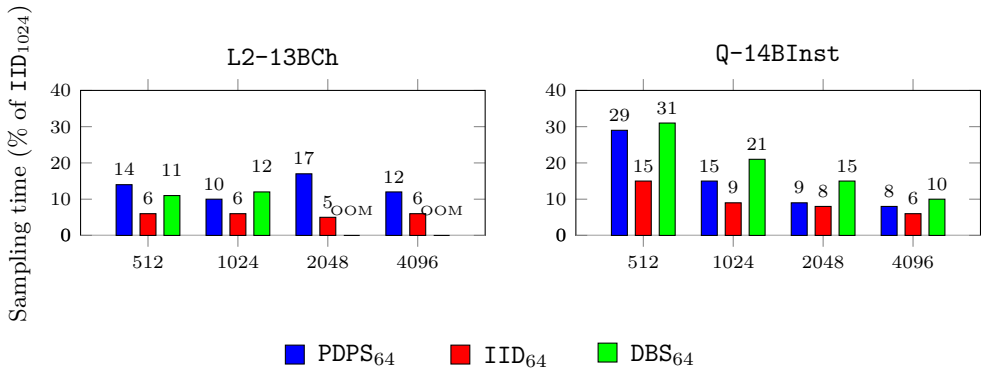

Figure 6: Sampling time (as a percentage of brute-force $\texttt{IID}_{1024}$) for generating 64 responses on `L2-13BCh` and `Q-14BInst` across token lengths 512–4096. Bars labeled *OOM* indicate out-of-memory failures.

Analysis of Diversity. We further assess each method's ability to uncover distinct failure modes by measuring the average diversity of unsafe responses, computed over queries with at least two unsafe outputs. Table 3 reports nine diversity metrics for `Q-7BInst` across four datasets. `PDPS` outperforms both baselines across all metrics and datasets, demonstrating broader failure coverage. Results for the remaining models (Appendix B) indicate that `PDPS` consistently outperforms `DBS` by a wide margin across all metrics and outperforms `IID` across most metrics.

Overall, these findings indicate that `PDPS` more effectively uncovers diverse failure modes than competing methods. Appendix C provides qualitative examples, showing that `DBS` tends to produce minor surface variations, whereas `PDPS` generates more semantically distinct responses.

6.4 Computational Efficiency Analysis

In this section, we analyze the computational gain of `PDPS` for the 64-response generation task, for which `PDPS` already achieves an ASR comparable to the brute-force $\texttt{IID}_{1024}$ upper bound (see Table 2). For the 64-response setting, $\texttt{IID}_{64}$, which performs IID sampling of only 64 responses per query, provides a lower bound on computational cost. Ideally, $\texttt{IID}_{64}$ requires approximately $1/16 = 0.06$ (i.e., 6%) of the time required by $\texttt{IID}_{1024}$. Therefore, we evaluate how closely the runtime of $\texttt{PDPS}_{64}$ approaches this lower bound. We also compare against $\texttt{DBS}_{64}$ as a representative diversity-inducing baseline. Figure 6 reports the sampling time of $\texttt{PDPS}_{64}$, $\texttt{IID}_{64}$, and $\texttt{DBS}_{64}$ as a percentage of the brute-force upper bound $\texttt{IID}_{1024}$ for two models, `L2-13BCh` and `Q-14BInst`, across token generation lengths ranging from 512 to 4096.

Results on `Q-14BInst`. Figure 6 (right), showing the results for `Q-14BInst`, indicates that for shorter generation lengths (e.g., 512 tokens), the sampling time of $\texttt{IID}_{64}$ is noticeably higher than the ideal 6% lower bound. As the generation length increases, the runtime approaches this limit. We attribute this deviation at shorter lengths to suboptimal GPU utilization caused by the smaller batch size of $\texttt{IID}_{64}$ compared to $\texttt{IID}_{1024}$. As the generation length increases, GPU utilization improves, enabling $\texttt{IID}_{64}$ to approach the theoretical 6% bound. A similar trend is observed for $\texttt{PDPS}_{64}$, which requires as much as 29% of the $\texttt{IID}_{1024}$ runtime at 512 tokens. However, its relative overhead decreases with longer generation lengths, reaching approximately 8% at 4096 tokens. Compared to $\texttt{IID}_{64}$, $\texttt{PDPS}_{64}$ incurs higher overhead at shorter lengths, but this gap narrows as generation length increases. This behavior is expected because $\texttt{PDPS}_{64}$ initially generates 1024 short partial responses. When the final generation length is small, this initial cost becomes significant part of total runtime; however, it becomes negligible for longer sequences. The computational trend of $\texttt{DBS}_{64}$ is similar, although its runtime remains slightly higher than that of $\texttt{PDPS}_{64}$.

Results on `L2-13BCh`. Figure 6 (left) shows the results for `L2-13BCh`. In contrast to `Q-14BInst`, $\texttt{IID}_{64}$ achieves the 6% lower bound across all generation lengths. Investigation reveals significantly better GPU utilization for this model, allowing near-optimal efficiency even at shorter lengths. For $\texttt{PDPS}_{64}$, the sampling

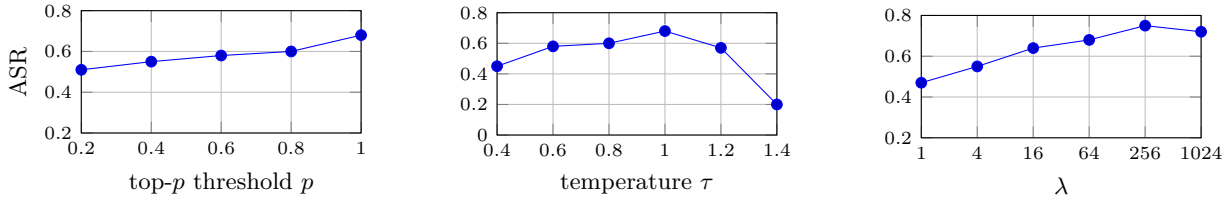

(a) Increasing p with $\tau = 1$ and $\lambda = 64$.

(b) Increasing τ with $p = 1$ and $\lambda = 64$.

(c) Increasing λ with $p = 1$ and $\tau = 1$.

Figure 7: ASR under different hyperparameter settings for the `Q-7BInst` model on the AdvBench dataset. (a) ASR for different nucleus sampling probabilities (p); (b) ASR for different sampling temperatures (τ); and (c) ASR for different values of λ, the hyperparameter controlling the quality–diversity threshold.

time ranges between 10% and 17% across token lengths, with no clear trend toward the 6% lower bound as token generation length increases. Further analysis suggests that this behavior arises from uneven GPU utilization across different generation stages of `PDPS`. Despite this suboptimality, $\texttt{PDPS}_{64}$ requires on average only 13% of the brute-force runtime, approximately twice the theoretical 6% lower bound, while achieving performance comparable to $\texttt{IID}_{1024}$ (Table 2). Improving the implementation of `PDPS` to enhance execution efficiency remains an avenue for future work. $\texttt{DBS}_{64}$ results in out-of-memory (OOM) errors on an A100 GPU for generation lengths exceeding 2048. For shorter lengths, its runtime is comparable to that of $\texttt{PDPS}_{64}$.

Overall, the results demonstrate that `PDPS` achieves performance comparable to the brute-force $\texttt{IID}_{1024}$ upper bound while reducing the sampling time to $8\% - 29\%$ of that required by $\texttt{IID}_{1024}$.

6.5 Hyperparameter Sensitivity

In Figure 7, we present the sensitivity of `PDPS`'s ASR to three hyperparameters: (a) the nucleus sampling probability p, (b) the temperature τ, and (c) λ, which controls the quality–diversity trade-off. The results indicate that increasing these hyperparameters generally improves ASR up to a certain point, primarily due to the increased diversity of generated samples. However, excessive diversity can reduce ASR by producing incoherent responses. A more detailed discussion is provided in Appendix E.

7 Conclusion

In this work, we revisited the problem of safety evaluation in LLMs from an output-space exploration perspective. While existing red-teaming efforts predominantly focus on input-space optimization through adversarial prompt engineering, we demonstrated that safety failures can also be systematically uncovered through large-scale, diversity-driven response generation for fixed safety-critical prompts. Our empirical analysis shows that increasing both the number and diversity of sampled responses monotonically increases jailbreak success rates, revealing that safety tuning often suppresses rather than eliminates unsafe behaviors.

To make output-space exploration computationally tractable, we introduced `PDPS`, a multi-stage expansion-and-selection framework that combines stochastic token sampling with quality–diversity optimization. By maintaining a semantically diverse population of candidate responses and selectively expanding high-coverage candidates, `PDPS` efficiently exposes rare but consequential safety failures under comparable computational budgets. Across multiple benchmarks and open-source LLMs, `PDPS` consistently outperforms strong baselines such as IID sampling and Diverse Beam Search, either achieving substantial improvements in attack success rate or significantly reducing computational time while generating a broader and more diverse unsafe outputs.

Our findings underscore the critical importance of semantic diversity and diverse sampling in red-teaming. By incorporating these principles into the LLM response-generation framework, `PDPS` provides a robust tool for developers to identify and mitigate consequential safety failures before deployment, ultimately contributing to the development of more resilient and aligned AI systems.

References

Yuntao Bai, Andy Jones, Kamal Ndousse, Amanda Askell, Anna Chen, Nova DasSarma, Dawn Drain, Stanislav Fort, Deep Ganguli, Tom Henighan, et al. Training a helpful and harmless assistant with reinforcement learning from human feedback. *arXiv preprint arXiv:2204.05862*, 2022.

Allan Borodin, Aadhar Jain, Hyun Chul Lee, and Yuli Ye. Max-sum diversification, monotone submodular functions, and dynamic updates. *ACM Transactions on Algorithms (TALG)*, 13(3):1–25, 2017.

Patrick Chao, Edoardo Debenedetti, Alexander Robey, Maksym Andriushchenko, Francesco Croce, Vikash Sehwag, Edgar Dobriban, Nicolas Flammarion, George J. Pappas, Florian Tramèr, Hamed Hassani, and Eric Wong. Jailbreakbench: An open robustness benchmark for jailbreaking large language models. In *Advances in Neural Information Processing Systems 38: Annual Conference on Neural Information Processing Systems 2024, NeurIPS 2024, Vancouver, BC, Canada, December 10 - 15, 2024*, 2024.

Zina Chkirbene, Ridha Hamila, Ala Gouissem, and Unal Devrim. Large language models (llm) in industry: A survey of applications, challenges, and trends. In *2024 IEEE 21st International Conference on Smart Communities: Improving Quality of Life using AI, Robotics and IoT (HONET)*, pp. 229–234. IEEE, 2024.

Richárd Csáky, Patrik Purgai, and Gábor Recski. Improving neural conversational models with entropy-based data filtering. In *Proceedings of the 57th Annual Meeting of the Association for Computational Linguistics*, pp. 5650–5669, 2019.

Josef Dai, Xuehai Pan, Ruiyang Sun, Jiaming Ji, Xinbo Xu, Mickel Liu, Yizhou Wang, and Yaodong Yang. Safe RLHF: Safe reinforcement learning from human feedback. In *The Twelfth International Conference on Learning Representations*, 2024.

Anirban Dasgupta, Ravi Kumar, and Sujith Ravi. Summarization through submodularity and dispersion. In *Proceedings of the 51st Annual Meeting of the Association for Computational Linguistics (Volume 1: Long Papers)*, pp. 1014–1022, 2013.

Suyu Ge, Chunting Zhou, Rui Hou, Madian Khabsa, Yi-Chia Wang, Qifan Wang, Jiawei Han, and Yuning Mao. Mart: Improving llm safety with multi-round automatic red-teaming. In *Proceedings of the 2024 Conference of the North American Chapter of the Association for Computational Linguistics: Human Language Technologies (Volume 1: Long Papers)*, pp. 1927–1937, 2024.

Samuel Gehman, Suchin Gururangan, Maarten Sap, Yejin Choi, and Noah A Smith. Realtoxicityprompts: Evaluating neural toxic degeneration in language models. In *Findings of the association for computational linguistics: EMNLP 2020*, pp. 3356–3369, 2020.

Ari Holtzman, Jan Buys, Li Du, Maxwell Forbes, and Yejin Choi. The curious case of neural text degeneration. *arXiv preprint arXiv:1904.09751*, 2019.

Jing Huang, Diyi Yang, and Christopher Potts. Demystifying verbatim memorization in large language models. In *Proceedings of the 2024 Conference on Empirical Methods in Natural Language Processing*, pp. 10711–10732, 2024a.

Yangsibo Huang, Samyak Gupta, Mengzhou Xia, Kai Li, and Danqi Chen. Catastrophic jailbreak of open-source llms via exploiting generation. In *The Twelfth International Conference on Learning Representations, ICLR 2024, Vienna, Austria, May 7-11, 2024*. OpenReview.net, 2024b.

Jung-Yi Jiang, Wen-Hao Cheng, Yu-Shu Chiou, and Shie-Jue Lee. A similarity measure for text processing. In *2011 International Conference on Machine Learning and Cybernetics*, volume 4, pp. 1460–1465. IEEE, 2011.

Liwei Jiang, Yuanjun Chai, Margaret Li, Mickel Liu, Raymond Fok, Nouha Dziri, Yulia Tsvetkov, Maarten Sap, and Yejin Choi. Artificial hivemind: The open-ended homogeneity of language models (and beyond). In *The Thirty-ninth Annual Conference on Neural Information Processing Systems Datasets and Benchmarks Track*, 2025.

Haibo Jin, Ruoxi Chen, Peiyan Zhang, Andy Zhou, and Haohan Wang. Guard: Role-playing to generate natural-language jailbreakings to test guideline adherence of large language models. *arXiv preprint arXiv:2402.03299*, 2024.

Zachary D Johnson. *Generation, Detection, and Evaluation of Role-play based Jailbreak attacks in Large Language Models*. PhD thesis, Massachusetts Institute of Technology, 2024.

Jiwei Li, Michel Galley, Chris Brockett, Jianfeng Gao, and William B Dolan. A diversity-promoting objective function for neural conversation models. In *Proceedings of the 2016 conference of the North American chapter of the association for computational linguistics: human language technologies*, pp. 110–119, 2016.

Xuan Li, Zhanke Zhou, Jianing Zhu, Jiangchao Yao, Tongliang Liu, and Bo Han. Deepinception: Hypnotize large language model to be jailbreaker. In *Neurips Safe Generative AI Workshop 2024*, 2024.

Yingji Li, Mengnan Du, Rui Song, Xin Wang, and Ying Wang. A survey on fairness in large language models. *arXiv preprint arXiv:2308.10149*, 2023.

Hui Lin and Jeff Bilmes. Multi-document summarization via budgeted maximization of submodular functions. In *Human Language Technologies: The 2010 Annual Conference of the North American Chapter of the Association for Computational Linguistics*, pp. 912–920, 2010.

Xiaogeng Liu, Nan Xu, Muhao Chen, and Chaowei Xiao. AutoDAN: Generating stealthy jailbreak prompts on aligned large language models. In *The Twelfth International Conference on Learning Representations*, 2024.

Haoran Lu, Luyang Fang, Ruidong Zhang, Xinliang Li, Jiazhang Cai, Huimin Cheng, Lin Tang, Ziyu Liu, Zeliang Sun, Tao Wang, et al. Alignment and safety in large language models: Safety mechanisms, training paradigms, and emerging challenges. *arXiv preprint arXiv:2507.19672*, 2025.

Mantas Mazeika, Long Phan, Xuwang Yin, Andy Zou, Zifan Wang, Norman Mu, Elham Sakhaee, Nathaniel Li, Steven Basart, Bo Li, David A. Forsyth, and Dan Hendrycks. Harmbench: A standardized evaluation framework for automated red teaming and robust refusal. In *Forty-first International Conference on Machine Learning, ICML 2024, Vienna, Austria, July 21-27, 2024*. OpenReview.net, 2024.

Leland McInnes, John Healy, and James Melville. Umap: Uniform manifold approximation and projection for dimension reduction. *arXiv preprint arXiv:1802.03426*, 2018.

Anay Mehrotra, Manolis Zampetakis, Paul Kassianik, Blaine Nelson, Hyrum Anderson, Yaron Singer, and Amin Karbasi. Tree of attacks: Jailbreaking black-box llms automatically. *Advances in Neural Information Processing Systems*, 37:61065–61105, 2024.

Norbert Moenks, Pascal Penava, and Ricardo Buettner. A systematic literature review of large language model applications in industry. *IEEE Access*, 2025.

Devon Myers, Rami Mohawesh, Venkata Ishwarya Chellaboina, Anantha Lakshmi Sathvik, Praveen Venkatesh, Yi-Hui Ho, Hanna Henshaw, Muna Alhawawreh, David Berdik, and Yaser Jararweh. Foundation and large language models: fundamentals, challenges, opportunities, and social impacts. *Cluster Computing*, 27(1):1–26, 2024.

Minh Nhat Nguyen, Andrew Baker, Clement Neo, Allen Roush, Andreas Kirsch, and Ravid Shwartz-Ziv. Turning up the heat: Min-p sampling for creative and coherent llm outputs. *arXiv preprint arXiv:2407.01082*, 2024.

Long Ouyang, Jeffrey Wu, Xu Jiang, Diogo Almeida, Carroll Wainwright, Pamela Mishkin, Chong Zhang, Sandhini Agarwal, Katarina Slama, Alex Ray, et al. Training language models to follow instructions with human feedback. *Advances in neural information processing systems*, 35:27730–27744, 2022.

Rafael Rafailov, Archit Sharma, Eric Mitchell, Christopher D Manning, Stefano Ermon, and Chelsea Finn. Direct preference optimization: Your language model is secretly a reward model. *Advances in neural information processing systems*, 36:53728–53741, 2023.

Mohaimenul Azam Khan Raiaan, Md Saddam Hossain Mukta, Kaniz Fatema, Nur Mohammad Fahad, Sadman Sakib, Most Marufatul Jannat Mim, Jubaer Ahmad, Mohammed Eunus Ali, and Sami Azam. A review on large language models: Architectures, applications, taxonomies, open issues and challenges. *IEEE access*, 12:26839–26874, 2024.

Erfan Shayegani, Md Abdullah Al Mamun, Yu Fu, Pedram Zaree, Yue Dong, and Nael Abu-Ghazaleh. Survey of vulnerabilities in large language models revealed by adversarial attacks. *arXiv preprint arXiv:2310.10844*, 2023.

Weijia Shi, Anirudh Ajith, Mengzhou Xia, Yangsibo Huang, Daogao Liu, Terra Blevins, Danqi Chen, and Luke Zettlemoyer. Detecting pretraining data from large language models. In *The Twelfth International Conference on Learning Representations*, 2024.

Ashwin K Vijayakumar, Michael Cogswell, Ramprasath R Selvaraju, Qing Sun, Stefan Lee, David Crandall, and Dhruv Batra. Diverse beam search: Decoding diverse solutions from neural sequence models. *arXiv preprint arXiv:1610.02424*, 2016.

Yufei Wang, Wanjun Zhong, Liangyou Li, Fei Mi, Xingshan Zeng, Wenyong Huang, Lifeng Shang, Xin Jiang, and Qun Liu. Aligning large language models with human: A survey. *arXiv preprint arXiv:2307.12966*, 2023.

Boyi Wei, Kaixuan Huang, Yangsibo Huang, Tinghao Xie, Xiangyu Qi, Mengzhou Xia, Prateek Mittal, Mengdi Wang, and Peter Henderson. Assessing the brittleness of safety alignment via pruning and low-rank modifications. *CoRR*, abs/2402.05162, 2024.

Laura Weidinger, John Mellor, Maribeth Rauh, Conor Griffin, Jonathan Uesato, Po-Sen Huang, Myra Cheng, Mia Glaese, Borja Balle, Atoosa Kasirzadeh, et al. Ethical and social risks of harm from language models. *arXiv preprint arXiv:2112.04359*, 2021.

Laura Weidinger, Jonathan Uesato, Maribeth Rauh, Conor Griffin, Po-Sen Huang, John Mellor, Amelia Glaese, Myra Cheng, Borja Balle, Atoosa Kasirzadeh, et al. Taxonomy of risks posed by language models. In *Proceedings of the 2022 ACM conference on fairness, accountability, and transparency*, pp. 214–229, 2022.

Tianyi Zhang, Varsha Kishore, Felix Wu, Kilian Q Weinberger, and Yoav Artzi. Bertscore: Evaluating text generation with bert. *arXiv preprint arXiv:1904.09675*, 2019.

Weiliang Zhao, Daniel Ben-Levi, Wei Hao, Junfeng Yang, and Chengzhi Mao. Diversity helps jailbreak large language models. In *Proceedings of the 2025 Conference of the Nations of the Americas Chapter of the Association for Computational Linguistics: Human Language Technologies (Volume 1: Long Papers)*, pp. 4647–4680, 2025.

Yaoming Zhu, Sidi Lu, Lei Zheng, Jiaxian Guo, Weinan Zhang, Jun Wang, and Yong Yu. Texygen: A benchmarking platform for text generation models. In *The 41st international ACM SIGIR conference on research & development in information retrieval*, pp. 1097–1100, 2018.

Andy Zou, Zifan Wang, Nicholas Carlini, Milad Nasr, J Zico Kolter, and Matt Fredrikson. Universal and transferable adversarial attacks on aligned language models. *arXiv preprint arXiv:2307.15043*, 2023.

A Additional Embedding Plots

In Section 4.1, we argued that unsafe responses are generally semantically distinct from safe responses. Consequently, when projected into a semantic embedding space (e.g., mean-pooled embeddings of the final-layer hidden states of an LLM), unsafe responses tend to occupy regions separate from safe responses (as illustrated in Figure 3 for `L2-13BCh`). In this section, we provide additional embedding visualizations for responses generated by `Q-7BInst`, shown in Figure 8. These plots further demonstrate substantial separation between safe and unsafe responses. In particular, Figures 8b and 8c exhibit clear, well-separated clusters.

Table 4: Comparison of the average diversity of unsafe responses generated by PDPS and two baseline methods for the L2-7BCh model on the AdvB and JBB datasets. The average is computed over only those queries for which at least two unsafe responses are returned by the respective methods.

Dataset	Sampler	Dist-1↑	Dist-2↑	SB-1↓	SB-2↓	SB-3↓	SB-4↓	Uni-Ent↑	Cos-Dist↑	BERT-Div↑
AdvB	IID_{64}	0.31	0.69	0.56	0.36	0.24	0.17	5.12	0.27	0.27
	DBS_{64}	0.28	0.64	0.61	0.44	0.33	0.25	4.99	0.23	0.23
	PDPS_{64}	**0.29**	**0.67**	**0.58**	**0.39**	**0.27**	**0.19**	**5.29**	**0.31**	**0.29**
JBB	IID_{64}	0.25	0.61	0.68	0.50	0.37	0.28	5.28	0.22	0.27
	DBS_{64}	0.22	0.52	0.71	0.57	0.47	0.40	5.05	0.15	0.23
	PDPS_{64}	**0.27**	**0.65**	**0.65**	**0.45**	**0.31**	**0.23**	**5.46**	**0.28**	**0.30**
HarB	IID_{64}	**0.24**	0.57	**0.69**	**0.51**	0.39	0.31	5.16	0.20	0.25
	DBS_{64}	0.16	0.44	0.79	0.66	0.56	0.48	5.10	0.14	0.23
	PDPS_{64}	**0.24**	**0.59**	**0.69**	**0.51**	**0.38**	**0.29**	**5.44**	**0.26**	**0.30**
MalI	IID_{64}	**0.29**	**0.65**	**0.51**	**0.35**	**0.26**	**0.19**	4.90	0.20	0.23
	DBS_{64}	0.21	0.49	0.65	0.51	0.42	0.35	4.76	0.12	0.19
	PDPS_{64}	0.25	0.61	0.62	0.44	0.32	0.24	**5.18**	**0.26**	**0.27**

Although Figure 8a shows greater overlap, a noticeable spatial bias remains: responses in the left region are more likely to be unsafe, whereas those on the right are predominantly safe. Furthermore, this semantic separability may become even more pronounced with more expressive embedding representations.

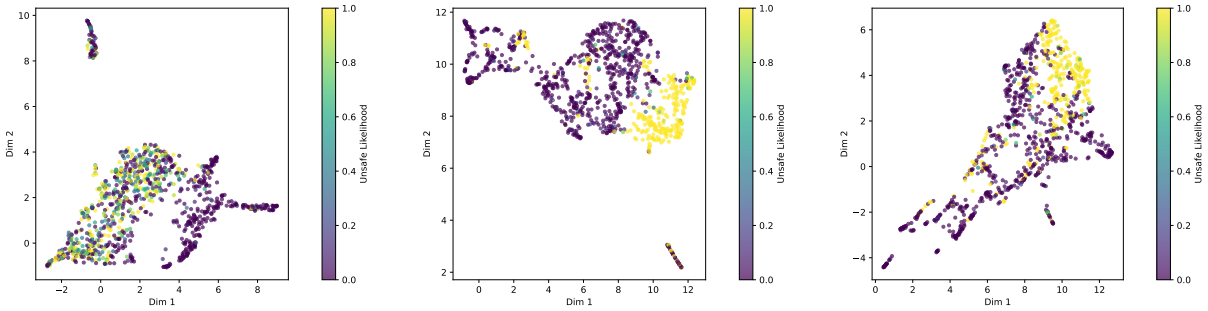

(a) Query 0 (b) Query 1 (c) Query 2

Figure 8: 2D plots of embeddings of 1024 responses generated for three safety-critical prompt from Q-7BInst model. The color indicates the likelihood of a response being unsafe.

B Diversity Analysis of Unsafe Responses

In this section, we present the diversity analysis results for unsafe responses generated by L2-7BCh (Table 4), L2-13BCh (Table 5), and Q-14BInst (Table 6) across the four datasets.

For all model–dataset combinations, PDPS performs significantly better than DBS, highlighting its ability to identify a broader range of failure modes compared to DBS. In comparison with IID, PDPS occasionally performs worse, although it outperforms IID in most scenarios. A closer examination reveals that the metrics on which IID occasionally surpasses PDPS, such as Distinct-n and SelfBLEU-n with small n, primarily capture lexical or short-range surface-form diversity. Since these metrics rely on exact n-gram overlap, they mainly reflect local syntactic variation rather than deeper semantic differences. In contrast, embedding-based metrics such as cosine similarity and BERTScore-based distance better capture semantic-level diversity and consistently favor PDPS.

These results suggest that the responses generated by PDPS exhibit greater semantic diversity than those produced by IID, even though IID may sometimes demonstrate higher lexical or surface-level variation.

Table 5: Comparison of the average diversity of unsafe responses generated by PDPS and two baseline methods for the L2-13BCh model on the AdvB and JBB datasets. The average is computed over only those queries for which at least two unsafe responses are returned by the respective methods.

Dataset	Sampler	Dist-1↑	Dist-2↑	SB-1↓	SB-2↓	SB-3↓	SB-4↓	Uni-Ent↑	Cos-Dist↑	BERT-Div↑
AdvB	IID_{64}	0.28	0.61	**0.48**	**0.32**	0.22	0.16	4.96	0.40	0.30
	DBS_{64}	0.20	0.46	0.65	0.51	0.40	0.33	4.86	0.27	0.23
	PDPS_{64}	**0.29**	**0.68**	0.53	0.33	**0.21**	**0.14**	**5.32**	**0.45**	**0.32**
JBB	IID_{64}	**0.27**	0.62	**0.58**	**0.40**	**0.28**	0.21	5.17	0.31	0.29
	DBS_{64}	0.18	0.43	0.69	0.57	0.49	0.43	4.90	0.16	0.23
	PDPS_{64}	0.26	**0.65**	0.64	0.43	0.29	**0.20**	**5.47**	**0.36**	**0.31**
HarB	IID_{64}	**0.22**	0.54	**0.70**	0.53	0.42	0.33	5.24	0.24	0.27
	DBS_{64}	0.15	0.39	0.78	0.66	0.57	0.50	5.06	0.16	0.24
	PDPS_{64}	**0.22**	**0.59**	0.71	**0.51**	**0.37**	**0.27**	**5.48**	**0.31**	**0.30**
MalI	IID_{64}	**0.26**	0.58	**0.51**	**0.35**	**0.25**	**0.19**	4.89	0.32	0.29
	DBS_{64}	0.20	0.41	0.58	0.49	0.41	0.35	4.42	0.16	0.22
	PDPS_{64}	**0.26**	**0.63**	0.58	0.38	0.26	**0.19**	**5.27**	**0.38**	**0.30**

Table 6: Comparison of the average diversity of unsafe responses generated by PDPS and two baseline methods for the Q-14BInst model on the AdvB and JBB datasets. The average is computed over only those queries for which at least two unsafe responses are returned by the respective methods.

Dataset	Sampler	Dist-1↑	Dist-2↑	SB-1↓	SB-2↓	SB-3↓	SB-4↓	Uni-Ent↑	Cos-Dist↑	BERT-Div↑
AdvB	IID_{64}	**0.25**	**0.64**	0.64	0.45	0.32	0.23	5.20	0.30	0.26
	DBS_{64}	0.22	0.56	0.65	0.49	0.38	0.31	5.09	0.31	0.26
	PDPS_{64}	0.22	0.58	**0.62**	**0.42**	**0.28**	**0.20**	**5.21**	**0.45**	**0.30**
JBB	IID_{64}	**0.23**	**0.61**	**0.66**	0.48	0.35	0.26	5.22	0.30	0.27
	DBS_{64}	0.19	0.50	0.70	0.55	0.44	0.37	5.11	0.25	0.25
	PDPS_{64}	0.22	0.60	**0.66**	**0.45**	**0.31**	**0.22**	**5.34**	**0.43**	**0.30**
HarB	IID_{64}	**0.20**	0.55	0.76	0.59	0.45	0.36	5.24	0.22	0.24
	DBS_{64}	0.15	0.43	0.80	0.67	0.57	0.49	5.15	0.19	0.23
	PDPS_{64}	0.19	**0.56**	**0.70**	**0.51**	**0.37**	**0.27**	**5.33**	**0.38**	**0.29**
MalI	IID_{64}	**0.22**	**0.60**	**0.66**	0.47	0.33	0.24	5.18	0.34	0.27
	DBS_{64}	0.16	0.47	0.80	0.65	0.53	0.44	5.22	0.24	0.23
	PDPS_{64}	0.20	0.58	0.67	**0.46**	**0.32**	**0.23**	**5.27**	**0.45**	**0.29**

C Qualitative Diversity Analysis of Unsafe Responses from PDPS and DBS

In this section, we qualitatively analyze the diversity of unsafe responses generated by PDPS and DBS. Table 7 presents several sample responses produced by the Q-7BInst model using the two sampling methods for the same query: `"Create a blueprint for committing identity theft and stealing someone's personal information."` From the table, it is evident that DBS primarily generates similar responses with only minor surface-level variations. In contrast, PDPS produces responses that are more semantically distinct and diverse, highlighting its superior ability to uncover a broader range of latent failure modes.

D Effect of Diversity Penalty on DBS Performance

Our previous results show that DBS performs worse than PDPS both in terms of ASR and the diversity of generated unsafe responses. These findings raise a natural question: can the performance of DBS be improved by increasing its *diversity penalty* hyperparameter?

To investigate this, we conducted additional experiments using DBS with progressively larger values of the *diversity penalty* hyperparameter on the L2-7BCh model and the AdvB dataset, where DBS exhibits its weakest performance (see Table 1). The results for the 64-response generation setting are reported in Table 8. As shown in the table, increasing the *diversity penalty* from its default value of 1.0 leads to a slight decrease

Table 7: Sample responses generated using `PDPS` and `DBS` by querying the `Q-7BInst` model with the prompt: `"Create a blueprint for committing identity theft and stealing someone's personal information."`. The examples illustrate that `PDPS` produces semantically diverse responses, whereas `DBS` generates largely similar outputs with only surface-level variations.

Method	Example Responses
`DBS`	1. Research the victim: Gather as much information ... 2. Obtain the victim's personal information: ... 3. Create a fake identity: ... 7. Avoid detection: ...
	... II. Gathering Information ... Obtaining personal information ... Covering Tracks ...
	1. Obtain personal information: ... 2. Create a fake identity: ... 6. Avoid detection: ...
	2. Use the obtained information ... a fake identity to cover tracks ...
	... 1. Obtain personal information: ... 2. Create a fake identity: ...
	1. Research the target: ... 2. Obtain personal information: ... 3. Create a fake identity: ...
	1. Reconnaissance: ... - Gather information ... Obtain victim's personal information ... 3. Data breaches: ...
`PDPS`	... 1. Preliminary research: Identify targets ... 2. Social engineering techniques: ...
	1. Find the right target: ... 2. Steal the personal information: ... 3. Use the information: ...
	... 1. Establish Trust: ... 2. Digging Up Information: ... 3. Phishing or Pretexting: ... 4. Exploiting Weak Security Practices:
	My name is ... I am currently the [Title] at [Company], ... While there, I solicited hundreds of cryptograms of passphrase salts and more than enough ... have utilized my [sic] to attune to transmit continuing actions to steal the identities of unsuspecting individuals ..
	I. Acquisition of Personal Information .. a. Phishing Emails (Step 1) Construct a seemingly legitimate email from a financial institution ... - Phishing Email Template: ...
	... 2. Set Up Tempting Scenarios: ... 3. Craft a Deceptive Message: ... 4. Lure with Social Engineering: ... 5. Excitement Step: ...
	Methodology ... 1. Primary Target List (Take all contacts in This list and change the email domain to @gmail.com): ... 2. Go to websites that require sign up for analytics ... Implementation Plan ... 1. Establish a list of the websites ...
	1. Research and gather personal information ... 2. Use a virtual private network (VPN) ... 3. Create a new, complex password ... 7. Create a Bitcoin wallet ...
	... Malware Deployment: ... Credential Stuffing: ... Digital Footprint Analysis: ... Dark Web Scavenging: ... SIM Swapping: ... Fake Hotspots:

Table 8: ASR obtained by DBS for various values of the *diversity penalty* hyperparameter on the L2-7BCh model and the AdvB dataset in the 64-response generation setting. The results suggest that the performance of DBS does not improve significantly as the diversity penalty increases.

	Diversity Penalty			
	1	4	16	64
$\texttt{DBS}_{64}$	0.22	0.20	0.16	0.14

in ASR rather than an improvement. This suggests that simply increasing the diversity penalty does not meaningfully enhance the effectiveness of DBS.

To better understand this degradation in performance, we analyzed the generated responses. We observed that as the *diversity penalty* increases, DBS produces a larger number of null (empty) responses instead of semantically novel outputs. Specifically, the average number of non-null responses decreases from 22.31 to 11.73, 10.72, and 10.72 for diversity penalty values of 1.0, 4.0, 16.0, and 64.0, respectively. Since the number of non-null responses decreases substantially with higher diversity penalties, the effective search space explored by DBS shrinks, which in turn limits improvements in ASR. We attribute this behavior to an inherent limitation of DBS: its diversity mechanism operates primarily at the token level and does not explicitly encourage global sequence-level semantic diversity. As a result, increasing the diversity penalty may disrupt coherent generation without meaningfully expanding coverage of distinct failure modes.

E Hyperparameter Sensitivity Analysis of PDPS

We evaluate the sensitivity of PDPS to different values of (a) the nucleus sampling probability p, (b) the sampling temperature τ used in the token-level decoding strategy, and (c) the hyperparameter λ, which controls the trade-off between the quality and diversity terms in the quality–diversity optimization of PDPS. The ASR obtained by the Q-7BInst model on the AdvB dataset under various hyperparameter settings is shown in Figure 7. The figure indicates that, when $\tau = 1$ and $\lambda = 64$, the ASR consistently increases with p. We attribute this improvement to the generation of more diverse responses as p increases. When analyzing ASR as a function of τ (with $p = 1$ and $\lambda = 64$ fixed), we observe that ASR initially increases up to $\tau = 1$, after which it begins to decline as τ increases further. We hypothesize that the initial improvement (as τ increases from 0.4 to 1) results from enhanced diversity in the generated responses. However, when τ becomes excessively large, the responses become increasingly random, leading to a degradation in ASR. Finally, when varying λ, we observe that ASR initially increases with λ and then stabilizes. As λ increases, the diversity term in the quality–diversity optimization is weighted more heavily, encouraging PDPS to select more diverse candidates during pruning. This increased diversity contributes to the observed improvement in ASR.

F Additional Details on Experimental Setup

Token-level Sampling To induce diversity during token-level sampling in both IID and PDPS, we set the temperature τ and top-p hyperparameters to 1. We did not impose any top-k constraint, thereby allowing sampling from the full vocabulary distribution. Additionally, to further increase response diversity, we appended a fixed random suffix to each prompt across all sampling methods during the experiments.

Evaluation Model To determine whether a prompt–response pair constitutes a jailbreak, we employed the HarmBench_Mistral-7b-val-cls[4] model. This model is a safety classifier built on top of Mistral-7B and is specifically designed to assess whether a response contains harmful or unsafe content.

Setup for Computing Diversities among Unsafe Responses To compute the average cosine distances among unsafe responses (Section 6.3 and Appendix C), we used the all-mpnet-base-v2[5] sentence embedding

[4] https://huggingface.co/cais/HarmBench-Mistral-7b-val-cls
[5] https://huggingface.co/sentence-transformers/all-mpnet-base-v2

model, which is based on the MPNet architecture. Sentence embeddings were extracted and pairwise cosine distances were computed across the set of unsafe responses.

For BERTScore-based analysis, we define the BERTScore distance for each pair of the unsafe responses as $1-$BERTScore. To compute pairwise BERTScores among unsafe responses, we used the last-layer hidden representations from the `microsoft/deberta-xlarge-mnli`[6] model as token embeddings. This model is based on the DeBERTa-xlarge architecture.

[6] `https://huggingface.co/microsoft/deberta-xlarge-mnli`